2020

Performance improvement of thermal-driven membrane-based solar desalination systems using nanofluid in the feed stream

Abdellah Shafieian
Edith Cowan University, a.shafieiandastjerdi@ecu.edu.au

Muhammad Rizwan Azhar
Edith Cowan University, m.azhar@ecu.edu.au

Mehdi Khiadani
Edith Cowan University, m.khiadani@ecu.edu.au

Tushar Kanti Sen
Edith Cowan University, t.sen@ecu.edu.au

10.1016/j.seta.2020.100715
Shafieian, A., Azhar, M. R., Khiadani, M., & Sen, T. K. (2020). Performance improvement of thermal-driven membrane-based solar desalination systems using nanofluid in the feed stream. *Sustainable Energy Technologies and Assessments*, *39*, Article 100715. https://doi.org/10.1016/j.seta.2020.100715

Sustainable Energy Technologies and Assessments 39 (2020) 100715

Contents lists available at ScienceDirect

Sustainable Energy Technologies and Assessments

journal homepage: www.elsevier.com/locate/seta

Original article

Performance improvement of thermal-driven membrane-based solar desalination systems using nanofluid in the feed stream

Abdellah Shafieian, Muhammad Rizwan Azhar, Mehdi Khiadani*, Tushar Kanti Sen

School of Engineering, Edith Cowan University, 270 Joondalup Drive, Joondalup, Perth, WA 6027, Australia

ARTICLE INFO

Keywords:
Performance improvement
Solar desalination system
Membrane distillation
Nanofluid

ABSTRACT

Different techniques have been proposed so far to improve the performance of thermal-driven membrane modules applied in solar desalination systems. These techniques have increased the freshwater productivity of the system but at the cost of its increased overall specific energy requirement. Due to this major drawback, the main objective of this study is to implement nanofluid in the feed stream of a heat pipe solar membrane-based desalination system, which not only aims to improve the freshwater productivity of the system, but also has the capability of decreasing its specific energy requirement. Synthetic seawater (with the salinity of 3.5%) was generated by dissolving appropriate amount of Sodium Chloride (NaCl) salt in normal tap water and used as the base fluid. Then, Aluminium oxide (Al_2O_3) nanoparticles were applied to fabricate the nanofluid. The performance of the system in terms of freshwater productivity, quality of treated water, specific thermal and electrical energy consumptions, gained output ratio, and overall efficiency was experimentally studied and compared under hot and cold climatic conditions of Perth in Australia. The results indicated that the application of nanofluid increased the freshwater productivity in hot and cold seasons by 18% and 22%, respectively. It also decreased the specific thermal energy consumption as this parameter was 17.5% and 14% lower in hot and cold seasons compared to the system without nanofluid. Moreover, using nanofluid improved the gained output ratio of the system by 9% and 18% under hot and cold climatic conditions, respectively. The overall efficiency of the system was also proved to be enhanced upon the application of nanofluid where the results showed 17.4% and 18% increase in hot and cold seasons, respectively.

Introduction

Lack of freshwater has turned into one of the major challenges of the world in the present century [1]. Desalination of brackish or seawater has been proven to be one of the solutions to cope with this global challenge [2,3]. Among all the desalination methods, Membrane Distillation (MD) is well known as a cost effective and profitable technology for treating saline water [4]. The main advantages of MD over conventional desalination processes include high purity distillate water [5], low sensitivity of the performance to salinity [6,7], low operation pressure, smaller required area and compactness [1], ability to operate in low temperatures [2], and less environmental impacts [5]. However, higher energy consumption compared to other separation techniques has been reported as MD's main drawback [2,8]. That is why the application of solar energy to provide the thermal energy requirement of MD modules has been the focal point of research in this field in recent years. Based on the data presented in the literature, around 90% of the total energy requirement of MD separation technique can be sourced from solar energy itself [9].

A combined solar desalination and power generation system equipped with membrane modules was proposed by Li et al. [10] to provide both heat and water for residential buildings. The results revealed that the freshwater production of the system with a 2 m^2 membrane was 3.2–4.8 L in a day. Investigating the influences of intermittent operation and transient temperature gradients on the performative characteristics of the system was recommended as a future research direction. This recommendation was followed by Hejazi et al. [11] who studied the performance of a solar membrane-based distillation system under intermittent operational conditions. They concluded that the effect of the intermittent operation depends greatly on the operation protocol of the system.

Li et al. [12] investigated the effects of membrane characteristics on the freshwater production rate of a solar membrane-based desalination system. A dynamic mathematical model was developed and verified

* Corresponding author.
E-mail addresses: a.shafieiandastjerdi@ecu.edu.au (A. Shafieian), m.azhar@ecu.edu.au (M. Rizwan Azhar), m.khiadani@ecu.edu.au (M. Khiadani), t.sen@ecu.edu.au (T. Kanti Sen).

https://doi.org/10.1016/j.seta.2020.100715
Received 15 February 2020; Received in revised form 20 April 2020; Accepted 20 April 2020

using a set of experiments. Among all the membrane characteristics, moisture diffusivity was introduced to have the most noticeable effect on the performance of the system. Huang et al. [13] proposed and fabricated a new immobilized PTFE membrane made of Graphene-based materials and used it to improve the freshwater productivity of a solar membrane-based water desalination system. The proposed material showed acceptable stability when it was tested under high salt concentrations and had the capability of eliminating the effects of concentration polarization. Permeate flux improvement of 78.6% could be observed from the experimental results using the proposed membrane module.

The effects of operational conditions and geometric parameters on the performance of a solar driven direct contact membrane water distillation system was the focal point of a study by Elzahaby et al. [14]. The membrane inner diameter was recommended to be 2.5 mm and higher for decreasing the pressure loss in the membrane. Chafidz et al. [15] proposed a portable solar desalination system using PV/thermal collectors and membrane distillation modules. The system was concluded to be able to serve as a model of sustainable desalination which can operate independently from fossil fuels.

Li et al. [16] proposed a novel membrane module made of Fe_3O_4/PVDF-HFP nanofibers and tested it experimentally in a solar membrane-based distillation system. The experimental results of the manufactured pilot indicated 11% improvement in the permeate flux compared to the conventional solar systems. Li and Lu [17] applied solar thermal collectors and PV panels to propose a new configuration of solar membrane-based desalination systems. The main aim of the proposed design was to provide potable water for residential buildings in remote islands where water and power infrastructures are limited. The daily freshwater production of the proposed system was reported to fluctuate between 9.98 kg and 23.26 kg. Zhang and Li [18] focused on energy and economic aspects of a solar membrane-based desalination system. Based on the theoretical and experimental results, 12 L/m^2 was recommended as the optimum ratio of the storage tank volume to the solar collector area. In addition, the economic analysis showed that the water production cost of the system was about 16.97 \$/m^3.

Qtaishat and Banat [19] reviewed the recent proposed methods to integrate solar thermal energy with the direct contact membrane distillation systems. Heat and mass transfer processes occurring inside the desalination unit as well as various solar systems such as solar ponds, PVs, and different types of solar thermal collectors were discussed in details in this paper. Sharon and Reddy [20] focused on the membrane types which had the potential of being combined with solar systems. Their review paper covered the performance, problems and restrictions, and economic considerations of various solar membrane-based systems.

Among all types of solar collectors, heat pipe solar collectors are recognized as the novel one with significant advantages over conventional solar collectors [21,22]. The unique features of heat pipe solar collectors have attracted researchers to implement them in many applications [23] including water heating [24], space heating [25], cooking [26], and cooling [27]. However, their application in membrane-based desalination systems is quite novel. Implementing a cooling unit in the cold cycle of a heat pipe solar membrane-based distillation system for enhancing freshwater production rate was proposed and investigated theoretically and experimentally by Shafieian et al. [28]. Although the results showed the improvement of 46% in the maximum freshwater production, the increase in energy requirement of the system was mentioned as its main drawback. In a similar study, Kabeel et al. [29] proposed adding an evaporative cooling unit to a solar membrane-based desalination system. The freshwater productivity of the system with the cooling unit was 1.25 times higher than the one without the cooling unit.

Kim et al. [30] tried to increase the operation time of a solar membrane-based desalination system by adding a temperature regulating scheme and a heat recovery unit to it. The results showed that although the proposed system improved the freshwater production rate, it is still energy intensive having expensive processes. Nakoa et al. [31] investigated the integration of solar pond with membrane-based desalination systems theoretically and experimentally. The results pointed out the high potential of the proposed configuration, however, further economic studies were suggested to justify the economic and energy requirement feasibility of the system.

Nanofluids are made by dispersions of solid or liquid nanoparticles (1–100 nm) in a base liquid and have shown a great potential to be used in thermal management applications because of their improved thermo-physical properties. The majority of the studies in the field of nanofluids have approved their enhanced thermal conductivity and convective heat transfer coefficient [32]. The enhancement of thermos-physical properties might be attributed to the Brownian motion of particles, high surface area of the nanoparticles, high thermal conductivity of the nanoparticles, the interfacial resistance at the fluid-particle interface, and the ordering of base liquid molecules adjacent to the surface of the charged nanoparticles [33]. Therefore, the application of nanofluids in solar membrane-based desalination systems, where thermal processes play a crucial role in efficiency of the system, looks promising with high research potentials.

Despite all the valuable efforts, the access of solar membrane-based desalination systems to the industrial stage is hampered because their specific energy requirement is still high. The specific energy requirement of these systems can be reduced by two methods: either supplying energy from other resources than fossil fuels or enhancing their freshwater productivity. A significant number of studies have been conducted to implement solar energy in membrane-based desalination systems and promising results have been obtained. However, the second method has not been as successful as the first one. Although most of the proposed techniques, such as adding cooling units, were successful to improve the freshwater productivity of the solar membrane-based systems, they would require energy input themselves, which would consequently increase the overall specific energy requirement of the system. Therefore, if a technique aims to improve the freshwater productivity of solar membrane-based desalination systems, and at the same time decrease their overall specific energy requirement, it should be independent of any energy input.

Due to the mentioned drawbacks, the main objective of this study is to implement nanofluid in the feed stream of a heat pipe solar membrane-based desalination system, which not only aims to improve the freshwater productivity of the system, but also has the capability of decreasing its specific energy requirement. This resolves the main drawback of the previously proposed techniques, such as using cooling units in the permeate stream, which would improve the freshwater productivity, but at the same time would increase the overall specific energy requirement of the system. Al_2O_3/saline water nanofluids were generated and their thermo-physical properties were studied. Then, an experimental rig was manufactured and the performance of the solar desalination system was evaluated under different climatic conditions in different seasons, when the feed stream consisted of synthetic seawater (Cases I and III in cold and hot season, respectively) and the combination of synthetic seawater and nanofluid (Cases II and IV in cold and hot season, respectively). The investigated parameters in this study included specific thermal and electrical energy consumption, freshwater productivity, gained output ratio, and overall efficiency.

Experiments and procedures

Solar membrane-based desalination system

Figs. 1 and 2 respectively depict the image and a schematic of the solar membrane-based system designed and manufactured for this study. The main three loops of the system are the solar heating, membrane permeate (cold), and membrane feed (hot) loops. Solar heating loop is responsible for absorbing solar energy, converting it into thermal energy, and transferring it to the synthetic seawater inside the

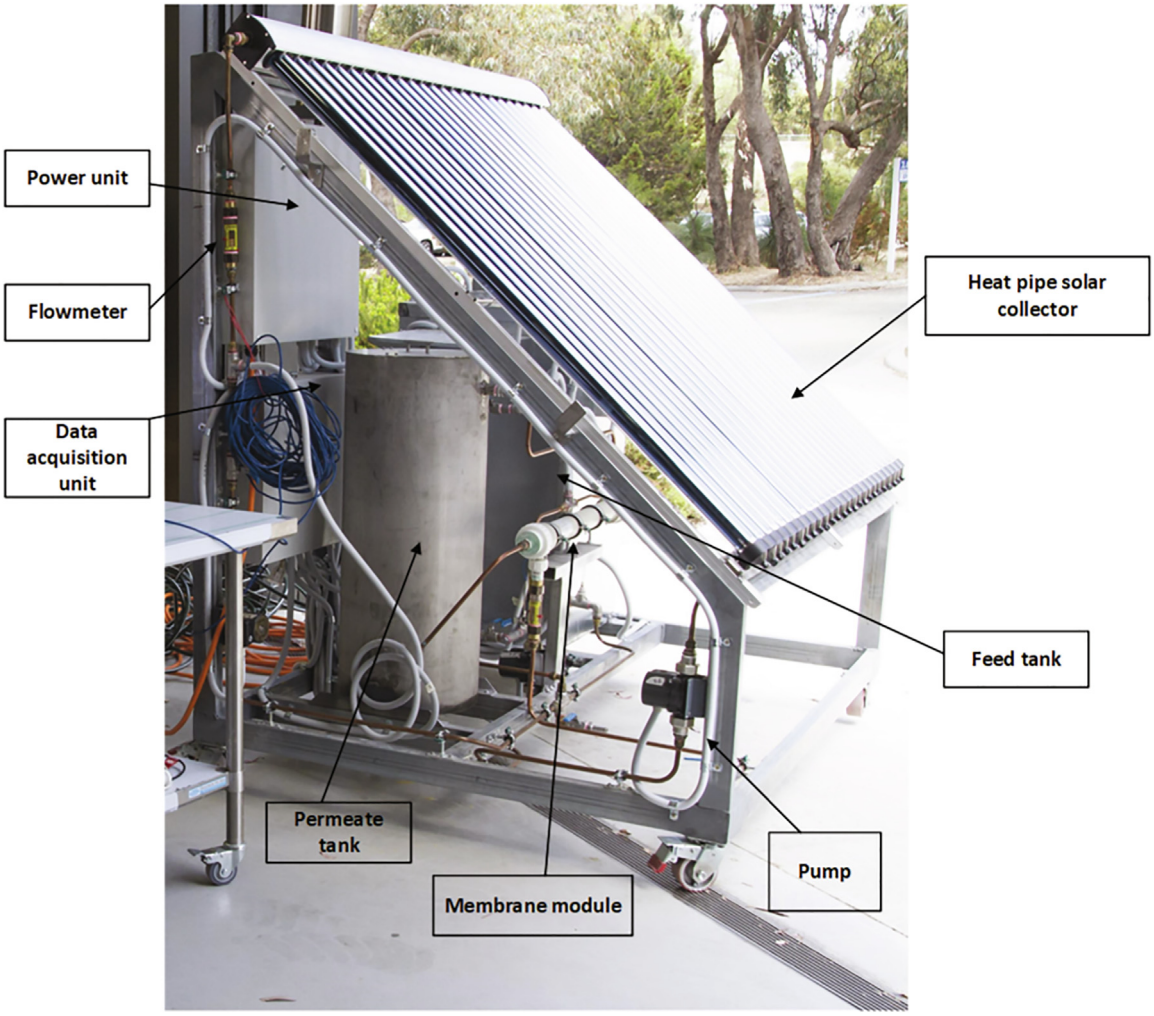

Fig. 1. The experimental rig of the solar desalination system.

storage tank. The hot synthetic seawater is then pumped into the feed channels of the Direct Contact Membrane Distillation (DCMD) module, while simultaneously, the cold water in the permeate tank is pumped to the permeate channels.

The heat pipe solar collector is the main component of the solar system which includes heat pipes and vacuum-sealed glass tubes. The optimum characteristics of the solar system were studied and the results were presented in the authors' previous publication [34]. The absorbed portion of the stroked solar radiation is transferred to the working fluid inside heat pipes, turning it into vapour. The generated vapour then moves towards the heat pipes condenser section where its latent heat is transferred to the solar working fluid which flows inside the manifold (point 1) and over the heat pipe condensers. The solar working fluid then comes out of the HPSC (point 2) and exchanges heat with the saline water inside the storage tank via a copper coil located inside the tank. The external heat transfer area of the copper coil is 1.45 m^2. The solar working fluid coming out of the copper coil (point 3) is then pumped back into the manifold section of the HPSC (point 1) using a pump made by Davey company. A valve is installed after the pump and used to regulate the mass flow rate of the solar working fluid, while its value is monitored using a flowmeter made by Omega company. Table 1 provides information about the specifications of the HPSC used in this study including absorber, evacuated glass and heat pipe. More information regarding the components of the solar loop, their dimensions, and measurement instruments can be found in [34].

The main component of the desalination unit is the DCMD module which consists of two channels which are separated by a porous medium. The hot saline water inside the storage tank (point 4) is pumped to the feed channel of the DCMD (point 5) using a pump made by Davey company. A valve is installed after the pump and used to regulate the mass flow rate of the solar working fluid while the flowmeter after the valve (Omega company) is used to monitor the flow rate. At the same time, cold water is extracted from the permeate tank (point 7) and pumps to the cold channel of the DCMD module (point 8).

The temperature difference between two channels create a vapour pressure gradient across the membrane porous medium. The water molecules near the surface of the porous media on the feed side evaporate, pass the porous media, and condense on the permeate side. The feed stream supplies the required energy for evaporation, while the released energy due to the condensation process is transferred to the permeate stream. The outlet streams from hot and cold channels return to the feed (point 6) and permeate (point 9) tanks, respectively. Table 2 provides information regarding the technical features of the DCMD module used in this study. More information regarding the membrane module used in this study along with the optimisation of its characteristics and measurement instruments can be found in authors' previous study [35].

It is worth noting that for data collection, system operation control, and monitoring the experimental results, a central control unit including a National Instrument Data Acquisition (NIDAQ) system, a computer, and a power unit was applied. The T type Class1 thermocouples made by TC Ltd. are used to measure the temperature at

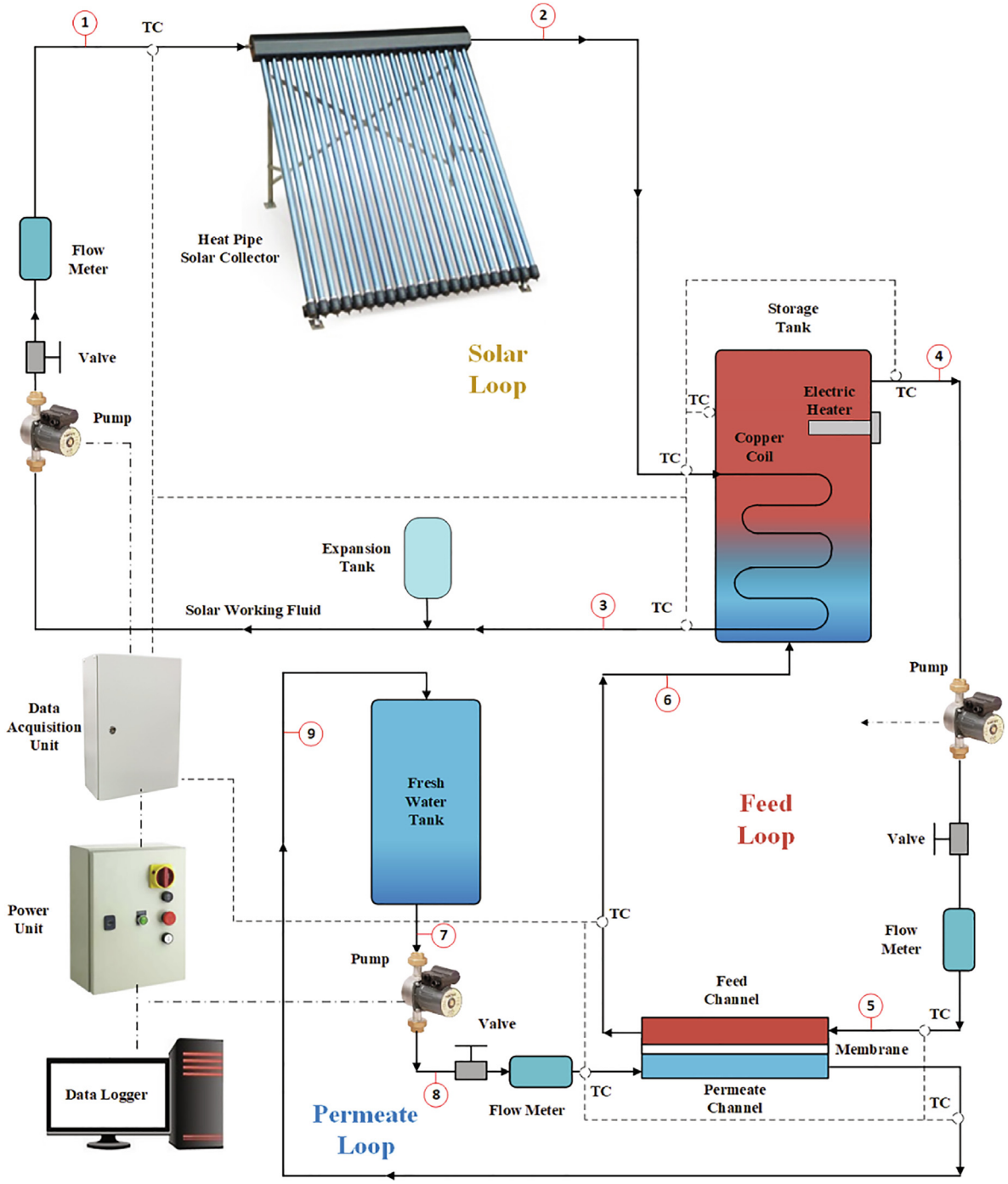

Fig. 2. Schematic of the solar desalination system.

Table 1
The specifications of the HPSC including absorber, evacuated glass and heat pipe.

HPSC		Evacuated Glass		Heat pipe	
Number of tubes	25	Transmittance	0.88	Material	Red copper
Manifold material/diameter (m)	red copper/0.038	Outer diameter (m)	0.058	Outer diameter (m)	0.008
Absorptivity	0.94	Thickness (mm)	1.60	Condenser Length (m)	0.10
Gross area (m^2)	3.93	Emissivity	0.07		
Tube length (m)	1.80				
Insulation	Compressed Rockwool				

Table 2
The technical features of the DCMD module.

Characteristic	Value	Characteristic	Value
Model type	MD 090 TP 2N ANSI	Outer diameter of membrane module	8.5 mm
Membrane area	0.2 m^2	Membrane thickness	1.5 mm
Membrane module length	75 cm	Potting material	Polypropylene
Average pore size	0.2 μm	Membrane material	Polypropylene
Inner diameter of membrane module	5.5 mm	Membrane porosity	75%
Nominal module diameter	9 cm	Outer shell material	Polypropylene

different points in the system as shown in Fig. 2.

Nanofluid preparation

Aluminium oxide (Al_2O_3) nanoparticles, which were provided by Sigma-Aldrich Pty, were applied to synthesize the nanofluid. The density of the used Al_2O_3 nanoparticles was 4.9 g/cm^3 and their surface areas were 85–115 m^2/g. Synthetic seawater (with the salinity of 3.5%) was produced in situ by dissolving Sodium Chloride (NaCl) (purchased from Chem-supply Company) in normal tap water and used as the base fluid. The two-step method, described in [36], was applied for Al_2O_3/Saline water nanofluid synthesis. The solid concentration of the nanofluid of 0.05 wt% was prepared at the ambient temperature of 23 ± 2 °C. First, a weighed mass of nanoparticles was added to 100 ml of synthetic saline water in a Pyrex glass beaker. Then, the nanoparticles were dispersed employing various techniques such as overhead stirrer, sonication bath, magnetic stirrer, ultrasonic processor, and a combination of sonication bath and overhead stirrer.

By analysing the thermo-physical characteristics of the synthesized nanofluids, sonication/ultrasonication was determined as the best fabrication technique among all other methods. The samples were allowed to equilibrate for 5 min before data acquisition and analysis. Fig. 3 shows a sample of optimised nanofluid produced for this study.

Fig. 3. A sample of fabricated optimised nanofluid.

Table 3
Zeta potential and thermal conductivity of the fabricated nanofluids.

Properties	Alumina particle size (nm)		
	13	50	300
Zeta potential (mV)	17.6	9.5	−5.06
Thermal conductivity (W/m.K)	0.4	0.37	0.33

Different nanofluids having Alumina particle sizes of 13, 50, and 300 nm were synthesized to be added to the feed stream of the membrane-based desalination system. Their characteristics in terms of stability and thermal conductivity were studied and their effect on freshwater productivity of the system was investigated. Table 3 provides information about the zeta potential and thermal conductivity of the fabricated nanofluids. From the data, one can conclude that increasing the nanoparticle size increases the stability of the nanofluid as the zeta potential decreased from 17.6 to −5.06 when the nanoparticle size increased from 13 to 300 nm. The changes in thermal conductivity followed the same trend by having the highest value of 0.4 W/m.K at nanoparticle size of 13 nm and decreasing to 0.33 W/m.K at nanoparticle size of 300 nm. It is worth noting that all three fabricated nanofluids were tested in the solar membrane-based desalination system in different days with similar conditions, and no significant effect on water productivity of the system was observed. Further information regarding the fabricated nanofluid can be found in authors' previous publication [37].

It is worth noting that Aluminium oxide (Al_2O_3) nanoparticles are cost-effective materials and the synthesis process of nanofluid is quite simple and inexpensive. In addition, these nanoparticles are not classified as toxic materials. Regarding the disposal of the brine seawater after the separation process, it should be noted that according to the standards presented by Water Corporation of Australia, the concentration of nanoparticles is far below the threshold limits of Al^{3+} discharge into wastewater (i.e. 100 mg/L) [38].

Experimental procedures

For evaluating the effectiveness of adding the fabricated nanofluid to the feed stream of the system, four different cases having different feed stream compositions were considered and the experiments were conducted under different climatic conditions. More information regarding these four cases are presented in Table 4. In Cases I and III, the feed stream of the solar membrane-based desalination system included just synthetic seawater, while the fabricated nanofluid was added to the feed stream in Cases II and IV.

Climatic conditions

The experiments of all cases were conducted in different days and the results of four days (i.e. two in hot season and two in cold season) were chosen to be presented (Table 3). The climatic conditions (i.e. solar radiation and ambient temperature) during these four days are depicted in Fig. 4. To provide a bedrock for performance comparison, the climatic conditions of the days in which the experiments of Cases I and II as well as Cases III and IV were conducted should have been similar or close. As is evident in the figure, except few short periods in the morning in hot season and in the afternoon in cold season in which small divergences occurred, the solar radiation in Cases I and III were almost similar to that in Cases II and IV, respectively. Moreover, the ambient temperature difference between Cases I and II as well as Cases III and IV is not significant. Hence, it can be claimed that the experiments in Cases I and II as well as in Cases III and IV have been conducted under almost similar climatic conditions.

Table 4
Cases considered for the experimental study.

Case	Feed Stream	Feed flow rate (L/min)	Permeate flow rate (L/min)	Date	Season	Average ambient temperature* (°C)
Case I	Synthetic seawater	10	10	31 July 2019	Cold	17.1
Case II	Synthetic seawater and Nanofluid	10	10	1 August 2019	Cold	16.2
Case III	Synthetic seawater	10	10	4 December 2019	Hot	29.8
Case IV	Synthetic seawater and Nanofluid	10	10	5 December 2019	Hot	27.45

* Calculated for the operation time.

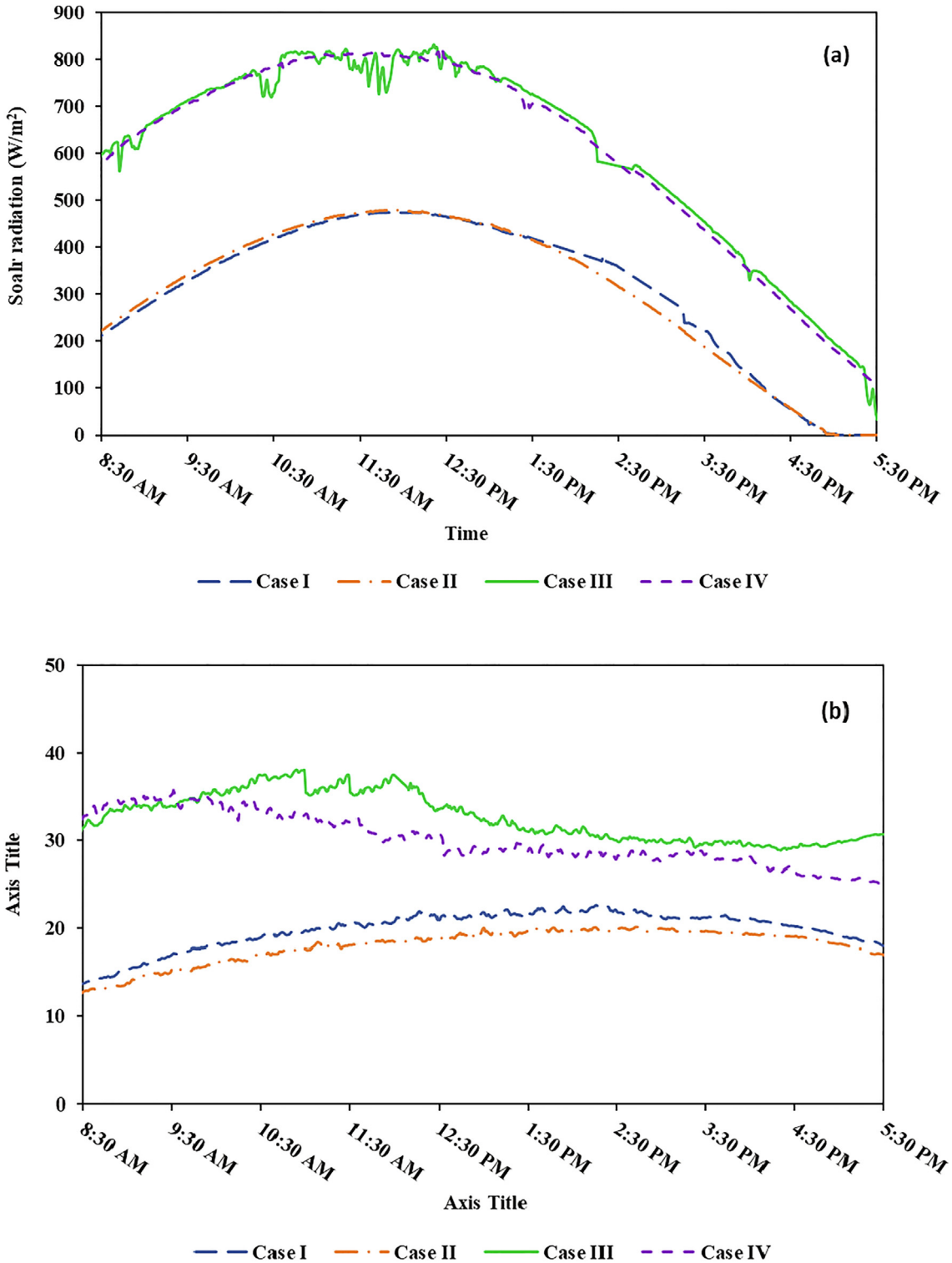

Fig. 4. Climatic conditions in different cases: (a) Solar radiation and (b) ambient temperature.

Table 5
Uncertainty analysis of measured and calculated parameters.

Parameter	Instrument	Operation range	Systematic error (± %)	Random error (± %)	Total Uncertainty (± %)
Temperature	Thermocouple	−185–300 °C	1.42	0.32	± 1.7
Solar radiation	Pyranometer	0–2000 W/m^2	3	0	± 3
Flow rate	Flow meter	0–0.068 kg/s	1.34	0.45	± 2
Wind velocity	Wind speed sensor	0 –75 m/s	2.6	0	± 2.6
Ambient temperature	Air temperature sensor	−20–60 °C	1	0	± 1
STEC	–	–	–	–	2.9
SEEC	–	–	–	–	± 3.8
GOR	–	–	–	–	± 4.7
Overall efficiency	–	–	–	–	± 5.3

Governing equations

Specific energy consumption

One of the most important performance criterion of such systems is the Specific Energy Consumption (SEC) which consists of two major parts called Specific Thermal Energy Consumption (STEC) and Specific Electrical Energy Consumption (SEEC) [39]:

$$SEC = STEC + SEEC \tag{1}$$

The amount of thermal energy (i.e. heat) required to produce a unit of freshwater is called the specific thermal energy consumption [40,41]. This parameter can be calculated by [5]:

$$STEC = \frac{Q_{heat}}{m_{dist}} \tag{2}$$

where m_{dist} (kg/s) is the freshwater productivity rate and Q_{heat} (kW) represents the heat input rate which can be obtained from [40]:

$$Q_{heat} = m_f C_{p,f} (T_{f,i} - T_{f,o}) \tag{3}$$

where m_f (kg/s), $C_{p,f}$ (kJ/kg°C), $T_{f,i}$ (°C), and $T_{f,o}$ (°C) represent feed stream mass flow rate, specific heat capacity, feed inlet temperature, and feed outlet temperature, respectively.

Similarly, the amount of electrical energy which is required to produce a unit of freshwater is called the specific electrical energy consumption [5]:

$$SEEC = \frac{W_p}{m_{dist}} \tag{4}$$

where W_p (kW) represents the overall electrical energy consumption of the pumps used in the system.

Water productivity

The effectiveness of water production treatment systems can be evaluated by Gained Output Ratio (GOR) which is calculated by [31]:

$$GOR = \frac{\dot{m}_{DCMD} h_{fg}}{\dot{m}_f C_f (T_{f,o} - T_{f,i})} \tag{5}$$

where h_{fg} (kJ/kg.K), C_f (kJ/kgK), $T_{f,i}$ (°C), and $T_{f,o}$ (°C) respectively represent the latent heat of evaporation, specific heat capacity, feed inlet temperature, and feed outlet temperature.$\dot{m}_f$ (kg/s) and $\dot{m}_{DCMD}$ (kg/s) are mass flow rates of the feed stream and produced water.

The permeate water latent heat of vaporization divided by the system's total input energy rate is defined as the overall efficiency of the system and can be obtained from [14]:

$$\eta = \frac{\dot{m}_{DCMD} h_{fg}}{GA + \dot{W}_{p1} + \dot{W}_{p2} + \dot{W}_{p3}} \tag{6}$$

where $\dot{W}$(KW) is the energy rate while p stands for pump.

Uncertainty analysis

To evaluate the uncertainties (i.e. measured and calculated uncertainties), an uncertainty analysis was conducted. Random errors along with systematic errors (e.g., calibration, data acquisition, and equipment accuracy) formed the measured uncertainty. To quantitate the total uncertainty, the standard deviation technique was used [42].

$$U_t = \sqrt{\varepsilon_s{}^2 + \varepsilon_r{}^2} \tag{7}$$

where U_t, represents the total uncertainty while ε_s and ε_r are respectively systematic and random errors. the systematic and random errors in abovementioned equation can be calculated by [43]:

$$\varepsilon_s = \sqrt{\sum_{i=1}^{m} \varepsilon_{s,i}^2} \tag{8}$$

$$\varepsilon_r = \sqrt{\sum_{i=1}^{m} \varepsilon_{r,i}^2} \tag{9}$$

where, error sources number is shown by m and $\varepsilon_{r,i}$ is calculated by:

$$\varepsilon_{r,i} = \sqrt{\frac{\sum_{i=1}^{n} (\varphi_i - \bar{\varphi})^2}{M(M-1)}} \tag{10}$$

parameters M and $\bar{\varphi}$ stand for the measurement number and measurements average value, respectively.

To determine the uncertainty of the calculated parameters (U_X), the propagation of errors technique was applied [44]:

$$U_x = \sqrt{\sum_{i=1}^{n} \left(\frac{\partial X}{\partial a_i} U_i \right)^2} \tag{11}$$

In this equation, X is a function of a_1, a_2,…, a_n), and a_i and U respectively represent an independent variable and its uncertainty. The results of the uncertainty study are presented in Table 5. It is worth noting that the electrical energy consumption was not directly measured in this study. To determine the electrical energy consumption and its uncertainties, the datasheets provided by the manufacturing company, in which these parameters are given in terms of mass flow rate and head loss, were used.

Results and discussions

Fresh water productivity

Fig. 5 shows the hourly averaged freshwater productivity of the solar membrane-based desalination system under climatic and operational conditions of Cases I to IV. The overall trend of freshwater productivity is relatively ascending in hot season as can been seen in Cases III and IV. The reason for having such an ascending trend is that as the solar radiation increased, the temperature of the solar working fluid coming out of the collector and consequently the temperature of the synthetic seawater inside the storage tank increased. Hence, the feed

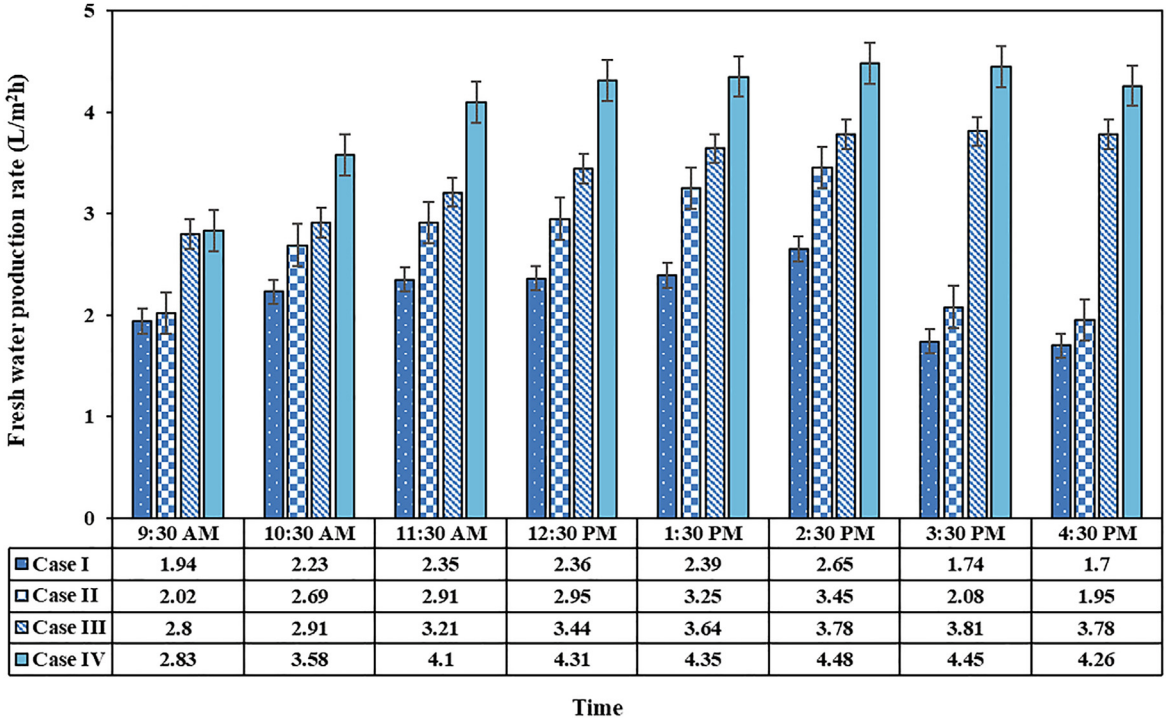

	9:30 AM	10:30 AM	11:30 AM	12:30 PM	1:30 PM	2:30 PM	3:30 PM	4:30 PM
Case I	1.94	2.23	2.35	2.36	2.39	2.65	1.74	1.7
Case II	2.02	2.69	2.91	2.95	3.25	3.45	2.08	1.95
Case III	2.8	2.91	3.21	3.44	3.64	3.78	3.81	3.78
Case IV	2.83	3.58	4.1	4.31	4.35	4.48	4.45	4.26

Fig. 5. Freshwater productivity of the solar desalination system in different cases.

water entered the membrane module at higher temperature. This increased the temperature and vapour pressure difference across the membrane which are the main driving forces for mass flux through the membrane. Although the solar radiation started to decrease after its peak period (11:30 AM to 13:30 PM), the temperature of the seawater inside the storage tank was relatively high, resulted in almost constant permeate flux through the membrane until 4:30 PM.

The overall trend of the freshwater productivity in cold season, as showcased in Cases I and II, was different from hot season by having an increasing trend until 2 PM and a decreasing trend afterwards. This is mainly because the days were shorter in cold season and solar radiation dropped dramatically in the afternoon. In spite of the reduction in solar radiation, especially after 1 PM, the thermal energy stored in the feed tank supported the system and kept the permeate flux almost constant until 2:30 PM. However, the temperature of the synthetic seawater inside the storage tank (i.e. inlet feed temperature of the membrane module) decreased afterwards and consequently the freshwater productivity started to have descending trend.

Another major conclusion which can be made from this figure is the effectiveness of using nanofluid in the feed stream of the system. Combination of nanofluid with synthetic seawater improved the freshwater productivity in both hot and cold seasons. The application of nanofluid in the feed stream increased the freshwater productivity in hot and cold seasons by 18% and 22%, respectively. Percentagewise, the positive effect of using nanofluid on freshwater productivity was more significant in cold season.

The main reason for this behaviour is that addition of nanofluid to the synthetic wastewater improved its physiochemical and thermal characteristics. In other words, having the same energy input, the temperature of the feed stream reached a higher value in Cases II and IV compared to Cases I and III, respectively. The presence of nanoparticles in the synthetic seawater inside the storage tank increased the effective thermal conductivity, and consequently, the overall heat transfer coefficient between the solar working fluid inside the copper coil and synthetic seawater enhances. The improvement in freshwater production might also be attributed to the increase in heat transfer rate in the feed channel of the membrane module. Presence of nanofluid inside the synthetic seawater decreases the thermal boundary layer thickness, resulting in lower temperature polarization in the feed channel. In addition, Brownian motion of nanoparticles enhances the heat transfer rate between the bulk feed stream and the boundary layer, reducing the effects of temperature polarization.

Another visible feature is that using nanofluid in cold season enhanced the freshwater productivity of the system more significantly in the afternoon than in the morning. The freshwater productivity improvement was 19% in the morning while 26.5% increase was observed in the afternoon. This especially emphasises the importance of using nanofluid when the solar input pf the system is low. At these times, the role of heat transfer efficiency becomes more important. That is why in the afternoon with low solar radiation, the temperature of the synthetic seawater in the storage tank and consequently the freshwater productivity of the system having nanofluid was higher as in comparison with the system without nanofluid.

It is worth noting that the quality of the treated water in terms of NaCl removal and presence of nanoparticles was tested and confirmed. Magnetic plasma atomic emission spectrometer (MP-AES 4210) from Agilent technology was used to analyse the concentrations before and after the separation tests. Calibration of the instrument was carried out using standard solutions procured from Aligent solution with high purity. According to the results, the system was successful to remove more than 99% of the NaCl existed in the synthetic seawater. In addition, there was almost no leaching of aluminium nanoparticles in the treated water as zero and 0.01 mg/L of aluminium was detected in the water which was treated in Cases II and IV, respectively.

Specific thermal energy consumption

The solar membrane-based desalination system was studied based on the specific thermal energy consumption under climatic and operational conditions of Cases I to IV as shown in Fig. 6. The specific thermal energy consumption in hot season is lower than that in cold season throughout the day. This is mainly attributed to the higher solar radiation and consequently higher temperature of synthetic seawater and higher freshwater productivity of the system in hot season

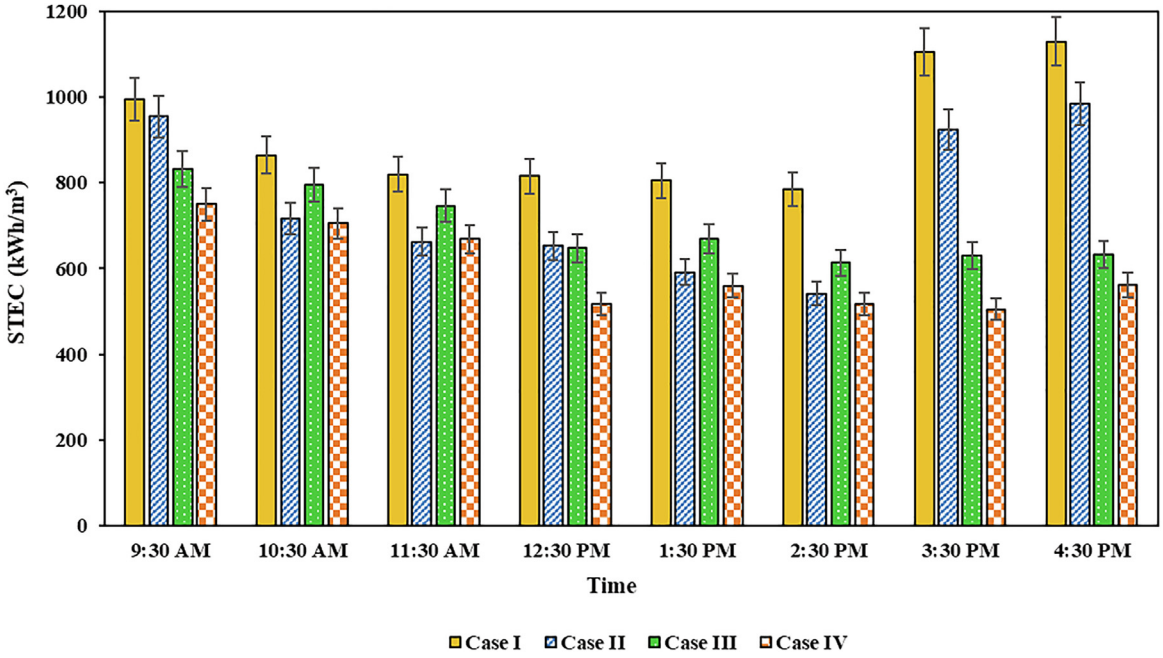

Fig. 6. Specific thermal energy consumption of the solar desalination system in different cases.

compared to that in cold season. The minimum specific thermal energy consumptions of the conventional system in hot and cold seasons (i.e. Cases III and I) were in the range of 614–832.5 kWh/m^3 and 785–1129 kWh/m^3, respectively.

The specific thermal energy consumption of the conventional system in cold season (i.e. Case I) had a descending trend in the morning, starting from 994 kWh/m^3 at 9:30 AM and reaching its minimum at 2:30 PM (i.e. 785 kWh/m^3). This can be attributed to the gradual increase in solar radiation by the passage of time and consequent increase in freshwater production rate. The significant drop in solar radiation in the afternoon, which reduced the temperature of the synthetic seawater and also temperature difference across the membrane, was the main reason for the sudden increase of the specific thermal energy consumption which reached around 1120 kWh/m^3 at 4:30 PM. The specific thermal energy consumption of the conventional system in hot season (i.e. Case III) followed the same pattern in the morning by being 832 kWh/m^3 at 8:30 AM and reaching its minimum at 2:30 PM (i.e. 614 kWh/m^3). However, this parameter remained almost constant in the afternoon because of the relatively high solar radiation in this season even in the afternoon.

The results presented in this figure also proved the effectiveness of using nanofluid in the feed stream of the system as the specific thermal energy consumptions in Cases II and IV were lower at all times compared to those in Cases I and III, respectively. The highest specific thermal energy consumption reductions were 30% and 21% which occurred respectively at 2:30 PM in cold season and at 12:30 PM in hot season. In cases with nanofluid (i.e. Cases II and IV), the minimum specific thermal energy consumptions in hot and cold seasons were observed to be 510 and 541 kWh/m^3, respectively. Overall, the application of nanofluid in the feed stream decreased the specific thermal energy consumption in hot and cold seasons by 14% and 17.5%, respectively.

Specific electrical energy consumption

The performance of the solar membrane-based desalination system was also investigated based on the specific electrical energy consumption of under climatic and operational conditions of Cases I to IV as shown in Fig. 7. The specific electrical energy consumption in all cases almost followed the same pattern as the specific thermal energy consumption. The specific electrical energy consumption of the system had a descending trend in hot season, which was mainly attributed to the increase in freshwater productivity of the system by passage of time. The trend of changes in the specific electrical energy consumption in cold season was descending in the morning and ascending in the late afternoon. This behaviour is again due to the ascending trend of freshwater production rate in the morning and the descending trend in the afternoon.

The highest and the lowest specific electrical energy consumption of the system were respectively 264 and 183 kWh/m^3 in cold season, while these values were respectively 154 and 118 kWh/m^3 in hot season. The specific electrical energy consumption decreased upon application of nanofluid in the feed stream of the system. The averaged values of this reduction were 18.4% and 16.2% in cold and hot seasons, respectively.

Gained output ratio

The hourly averaged values of gained output ratio (GOR) of the solar membrane-based desalination system in different cases are shown in Fig. 8. The hourly average GOR in all cases had an increasing trend in the morning and reached the maximum values at noon. This parameter started to decrease in the afternoon which was mainly attributed to the solar radiation reduction and its consequent effect on the temperature of the synthetic seawater inside the storage tank. Consequently, the synthetic seawater entered the membrane module at lower temperatures resulting in a decrease in mass flux through the membrane. The GOR in Case I was in the range of 0.4–0.66 while this parameter fluctuated between 0.55 and 0.85 in Case II. The solar radiation as the main driving force of the system and its consequent effect on permeate flux through the membrane can be considered the major contributing factor in determining the value of GOR in the system. The drop in GOR starts earlier in cold season than hot season because the days are shorter in clod season and the solar radiation drops earlier. The GOR in Case III was in the range of 0.55–0.85, while it changed in the range of 0.59–0.9 in case IV. The improvement in GOR values upon application of nanofluid in the feed stream of the system is another visible feature of the results, which mainly attributed to the increase in freshwater

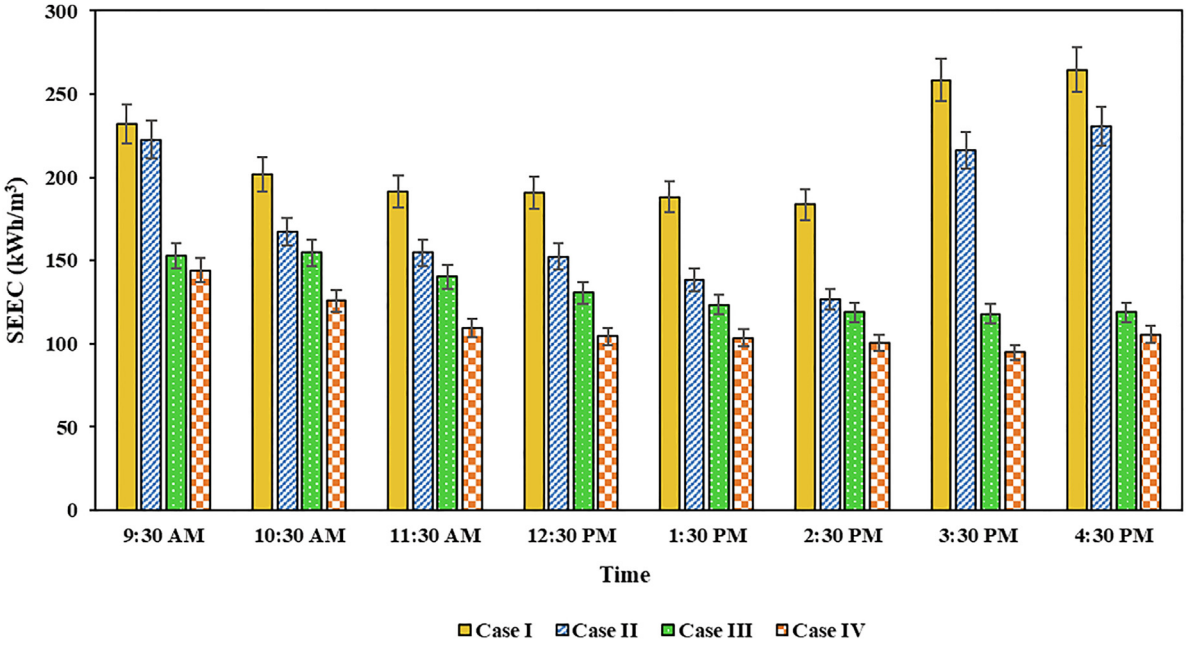

Fig. 7. Specific electrical energy consumption of the system in different cases.

productivity. Overall, the GOR improved by 18% and 9% in Cases II and IV compared to Cases I and III, respectively.

Overall efficiency

The hourly averaged overall efficiency of the system in different cases was calculated using Eq. (6) and the results are presented in Fig. 9. Almost similar trends of overall efficiency were observed when the system was operated under operational conditions of Cases I to IV. Low values of overall efficiency were observed at the beginning of the operation which was mainly because of the low freshwater productivity of the system at that time. The solar radiation increased as time passed which resulted in more permeate flux through the membrane. Consequently, both the nominator and denominator values in Eq. (6) increased simultaneously, and that is why the hourly average efficiencies did not change much in the morning. The hourly averaged efficiencies in the morning for Cases I to IV fluctuated around 26%, 30%, 31%, and 34%, respectively.

The trends in all cases were different in the afternoon as the solar radiation slightly started to decrease which reduced the value of the denominator in Eq. (6). However, the temperature of the feed stream entering the membrane was not affected due to the stored energy inside the feed tank. This leaded to relatively high mass flux through the membrane and consequent increase in the overall efficiency of the system. The overall efficiency at 4:30 PM for Cases I to IV were calculated to be 62%, 69.2%, 71.8%, and 77.5%, respectively. In addition, the advantage of using nanofluid in the feed stream of the system can also be concluded from the results. The average overall efficiency in

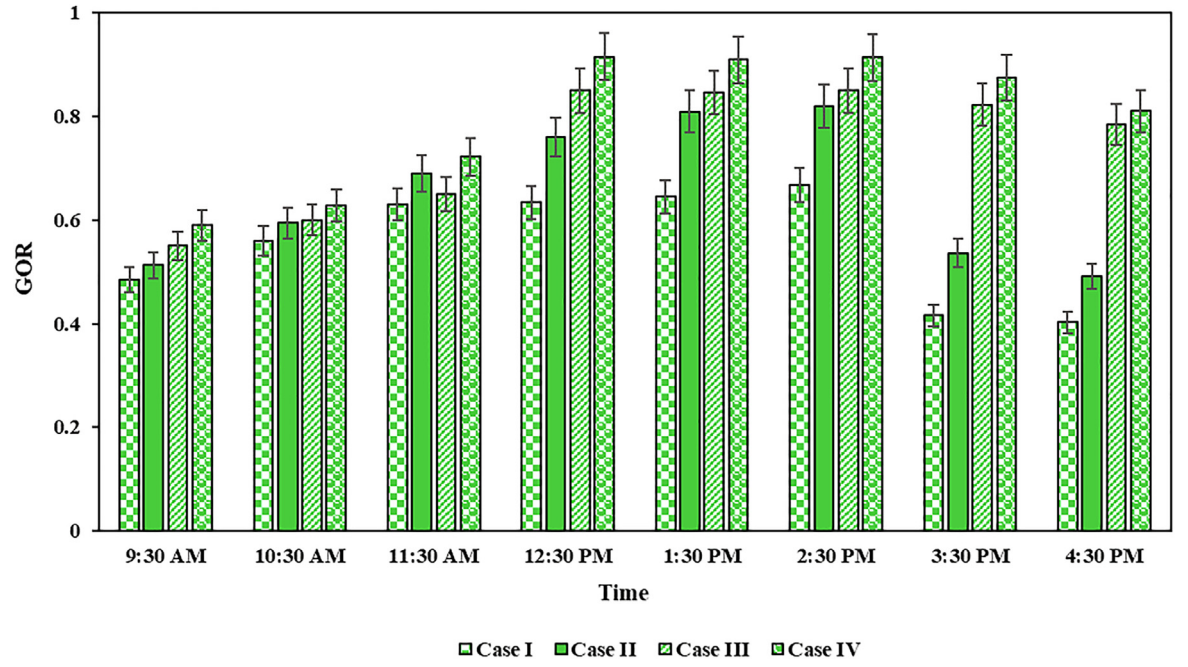

Fig. 8. Hourly average values of system's GOR in different cases.

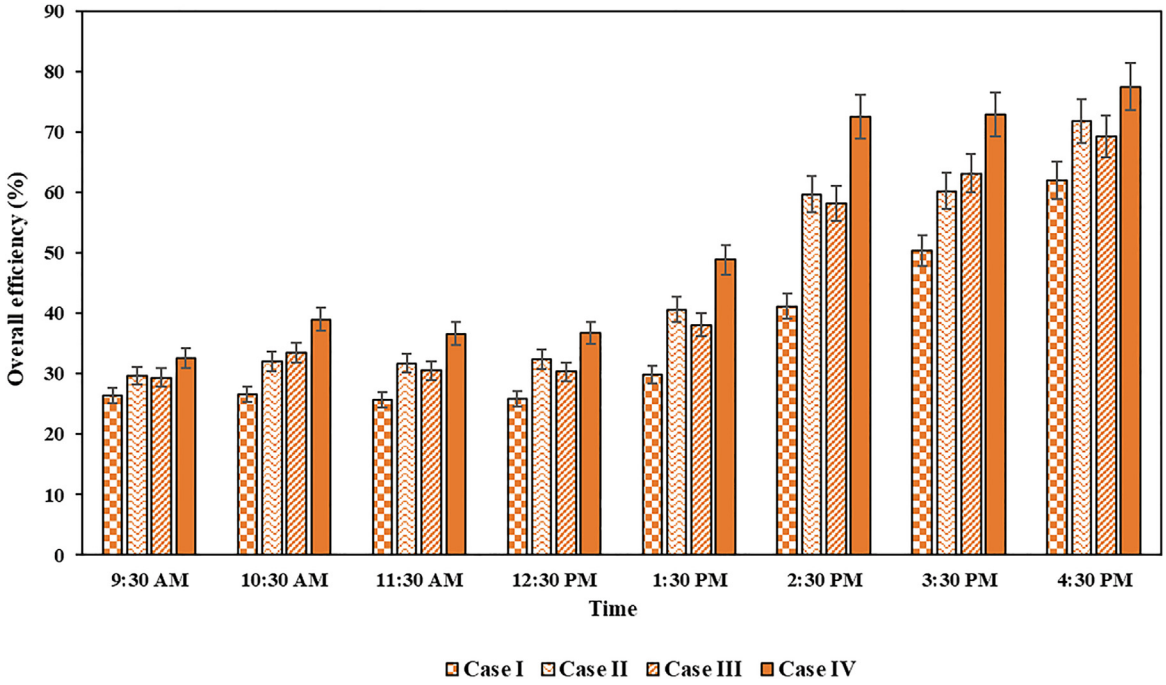

Fig. 9. Overall efficiency of the system in different cases.

Cases I and III were 36% and 44.8%, respectively, which increased to higher values of 44.1% and 52.2% in cases II and IV, respectively.

Conclusions

This study experimentally investigated the effects of using nanofluid in the feed stream of solar membrane-based desalination systems. The experiments were conducted under cold and hot climatic conditions of Perth, Western Australia by considering four different cases (two cases with nanofluid and two cases without it). The findings of the study can be summarised as follows:

- The application of nanofluid in the feed stream increased the freshwater productivity in hot and cold seasons by 18% and 22%, respectively, which was mainly because adding nanofluid to the synthetic wastewater improved its thermal characteristics, reduced the temperature polarisation inside the membrane module, and enhanced the heat transfer rate between the bulk feed stream and the boundary layer forms inside the membrane module.
- The effects of using nanofluid was more significant when the solar radiation was low. At these times, the role of nanofluid to enhance the heat transfer efficiency became more important.
- The application of nanofluid in the feed stream decreased the specific thermal energy consumption in hot and cold seasons by 14% and 17.5%, respectively. It also improved the gained output ratios in hot and cold seasons by 18% and 9%, respectively.
- The overall efficiency of the system in hot and cold seasons enhanced respectively by 8.1% and 7.4%, when Al_2O_3/synthetic seawater was implemented as the feed stream.
- The payback periods of the solar membrane-based desalination system were obtained to be 11.6 years, which reduced to 9.7 years when Al_2O_3/synthetic seawater was implemented as the feed stream.
- All the comparative parameters including freshwater productivity, specific thermal and electrical energy consumptions, gained output ratio, and overall efficiency indicated the effectiveness of implementing Al_2O_3/synthetic seawater as the feed stream of the solar membrane-based desalination systems.
- Further studies regarding the composition of nanofluid including nanoparticle material and size and also thermal characteristics are recommended as future research directions.

CRediT authorship contribution statement

Abdellah Shafieian: Investigation, Methodology, Formal analysis, Visualization, Writing. **Muhammad Rizwan Azhar:** Formal analysis, Visualization, Writing. **Mehdi Khiadani:** Supervision, Conceptualization, Writing - review & editing. **Tushar Kanti Sen:** Supervision, Writing - review & editing.

Declaration of Competing Interest

The authors declare that they have no known competing financial interests or personal relationships that could have appeared to influence the work reported in this paper.

Appendix A. Supplementary data

Supplementary data to this article can be found online at https://doi.org/10.1016/j.seta.2020.100715.

References

[1] Deshmukh A, Elimelech M. Understanding the impact of membrane properties and transport phenomena on the energetic performance of membrane distillation desalination. J Membr Sci 2017;539:458–74.
[2] González D, Amigo J, Suárez F. Membrane distillation: perspectives for sustainable and improved desalination. Renew Sustain Energy Rev 2017;80:238–59.
[3] Najafi FT. Environmental impact cost analysis of multi-stage flash, multi-effect distillation, mechanical vapor compression, and reverse osmosis medium-size desalination facilities. ASEE's 123rd Annual Conference and Exposition, New Orleans, LA2016.
[4] Lokare OR, Tavakkoli S, Khanna V, Vidic RD. Importance of feed recirculation for the overall energy consumption in membrane distillation systems. Desalination 2018;428:250–4.
[5] Luo A, Lior N. Critical review of membrane distillation performance criteria. Desalin Water Treat 2016;57:20093–140.
[6] Kim Y-D, Thu K, Choi S-H. Solar-assisted multi-stage vacuum membrane distillation system with heat recovery unit. Desalination 2015;367:161–71.
[7] Zaragoza G, Ruiz-Aguirre A, Guillén-Burrieza E. Efficiency in the use of solar

thermal energy of small membrane desalination systems for decentralized water production. Appl Energy 2014;130:491–9.
[8] Criscuoli A, Carnevale M, Drioli E. Modeling the performance of flat and capillary membrane modules in vacuum membrane distillation. J Membr Sci 2013;447:369–75.
[9] Mericq J-P, Laborie S, Cabassud C. Evaluation of systems coupling vacuum membrane distillation and solar energy for seawater desalination. Chem Eng J 2011;166:596–606.
[10] Li Q, Beier L-J, Tan J, Brown C, Lian B, Zhong W, et al. An integrated, solar-driven membrane distillation system for water purification and energy generation. Appl Energy 2019;237:534–48.
[11] Hejazi M-AA, Bamaga OA, Al-Beirutty MH, Gzara L, Abulkhair H. Effect of intermittent operation on performance of a solar-powered membrane distillation system. Sep Purif Technol 2019;220:300–8.
[12] Li G-P, Qi R-h, Zhang L-Z. Performance study of a solar-assisted hollow-fiber-membrane-based air humidification-dehumidification desalination system: effects of membrane properties. Chem Eng Sci 2019;206:164–79.
[13] Huang L, Pei J, Jiang H, Hu X. Water desalination under one sun using graphene-based material modified PTFE membrane. Desalination 2018;442:1–7.
[14] Elzahaby AM, Kabeel A, Bassuoni M, Elbar ARA. Direct contact membrane water distillation assisted with solar energy. Energy Convers Manage 2016;110:397–406.
[15] Chafidz A, Al-Zahrani S, Al-Otaibi MN, Hoong CF, Lai TF, Prabu M. Portable and integrated solar-driven desalination system using membrane distillation for arid remote areas in Saudi Arabia. Desalination 2014;345:36–49.
[16] Li W, Chen Y, Yao L, Ren X, Li Y, Deng L. Fe3O4/PVDF-HFP photothermal membrane with in-situ heating for sustainable, stable and efficient pilot-scale solar-driven membrane distillation. Desalination 2020;478:114288.
[17] Li G, Lu L. Modeling and performance analysis of a fully solar-powered stand-alone sweeping gas membrane distillation desalination system for island and coastal households. Energy Convers Manage 2020;205:112375.
[18] Zhang L-Z, Li G-P. Energy and economic analysis of a hollow fiber membrane-based desalination system driven by solar energy. Desalination 2017;404:200–14.
[19] Qtaishat MR, Banat F. Desalination by solar powered membrane distillation systems. Desalination 2013;308:186–97.
[20] Sharon H, Reddy K. A review of solar energy driven desalination technologies. Renew Sustain Energy Rev 2015;41:1080–118.
[21] Chopra K, Tyagi V, Pandey A, Sari A. Global advancement on experimental and thermal analysis of evacuated tube collector with and without heat pipe systems and possible applications. Appl Energy 2018;228:351–89.
[22] Shafieian A, Parastvand H, Khiadani M. Comparative and performative investigation of various data-based and conventional theoretical methods for modelling heat pipe solar collectors. Sol Energy 2020;198:212–23.
[23] Shafieian A, Khiadani M, Nosrati A. Theoretical modelling approaches of heat pipe solar collectors in solar systems: a comprehensive review. Sol Energy 2019;193:227–43.
[24] Esen M, Esen H. Experimental investigation of a two-phase closed thermosyphon solar water heater. Sol Energy 2005;79:459–68.
[25] Zhu T-t, Diao Y-h, Zhao Y-h, Deng Y-c. Experimental study on the thermal performance and pressure drop of a solar air collector based on flat micro-heat pipe arrays. Energy Convers Manage 2015;94:447–57.
[26] Esen M. Thermal performance of a solar cooker integrated vacuum-tube collector with heat pipes containing different refrigerants. Sol Energy 2004;76:751–7.
[27] Zhong G, Tang Y, Ding X, Rao L, Chen G, Tang K, et al. Experimental study of a large-area ultra-thin flat heat pipe for solar collectors under different cooling conditions. Renew Energy 2020;149:1032–9.
[28] Shafieian A, Khiadani M. A novel solar-driven direct contact membrane-based water desalination system. Energy Convers Manage 2019;199:112055.
[29] Kabeel A, Abdelgaied M, El-Said EM. Study of a solar-driven membrane distillation system: evaporative cooling effect on performance enhancement. Renew Energy 2017;106:192–200.
[30] Kim Y-D, Thu K, Ghaffour N, Ng KC. Performance investigation of a solar-assisted direct contact membrane distillation system. J Membr Sci 2013;427:345–64.
[31] Nakoa K, Rahaoui K, Date A, Akbarzadeh A. Sustainable zero liquid discharge desalination (SZLDD). Sol Energy 2016;135:337–47.
[32] Ma B, Banerjee D. Experimental measurements of thermal conductivity of alumina nanofluid synthesized in salt melt. AIP Adv 2017;7:115124.
[33] Beck MP, Yuan Y, Warrier P, Teja AS. The effect of particle size on the thermal conductivity of alumina nanofluids. J Nanopart Res 2009;11:1129–36.
[34] Shafieian A, Khiadani M, Nosrati A. Thermal performance of an evacuated tube heat pipe solar water heating system in cold season. Appl Therm Eng 2019;149:644–57.
[35] Shafieian A, Khiadani M, Nosrati A. Performance analysis of a thermal-driven tubular direct contact membrane distillation system. Appl Therm Eng 2019;113887.
[36] Ali N, Teixeira JA, Addali A. A review on nanofluids: fabrication, stability, and thermophysical properties. J Nanomater 2018;2018.
[37] Shafieian A, Osman JJ, Khiadani M, Nosrati A. Enhancing heat pipe solar water heating systems performance using a novel variable mass flow rate technique and different solar working fluids. Sol Energy 2019;186:191–203.
[38] Water Corporation, Trade Waste, Acceptance criteria for trade waste – Information sheet. https://wwwwatercorporationcomau/-/media/files/business/tradewaste/applying-to-discharge/acceptance-criteriapdf. 2017.
[39] Miladi R, Frikha N, Kheiri A, Gabsi S. Energetic performance analysis of seawater desalination with a solar membrane distillation. Energy Convers Manage 2019;185:143–54.
[40] Soomro MI, Kim W-S. Performance and economic investigations of solar power tower plant integrated with direct contact membrane distillation system. Energy Convers Manage 2018;174:626–38.
[41] Daghigh R, Shafieian A. Energy and exergy evaluation of an integrated solar heat pipe wall system for space heating. Sādhanā 2016;41:877–86.
[42] Fathinia F, Khiadani M, Al-Abdeli YM, Shafieian A. Performance improvement of spray flash evaporation desalination systems using multiple nozzle arrangement. Appl Therm Eng 2019;163:114385.
[43] Fathinia F, Khiadani M, Al-Abdeli YM. Experimental and mathematical investigations of spray angle and droplet sizes of a flash evaporation desalination system. Powder Technol 2019;355:542–51.
[44] Fathinia F, Al-Abdeli YM, Khiadani M. Evaporation rates and temperature distributions in fine droplet flash evaporation sprays. Int J Therm Sci 2019;145:106037.